



# Corneal confocal microscopy differentiates patients with secondary parkinsonism from idiopathic Parkinson's disease



Hong-Qi Yang<sup>1,2,7</sup>✉, Ran Xin<sup>3,7</sup>, Ning-Ning Che<sup>2,7</sup>, Qiu-Huan Jiang<sup>1</sup>, Shuai Chen<sup>1</sup>, Si-Yuan Chen<sup>1</sup>, Zhi-Kun Sun<sup>1</sup>, Wei-Min Yang<sup>4</sup>, Xue Li<sup>1</sup>, Jian-Jun Ma<sup>1</sup>, Jie-Wen Zhang<sup>1</sup>✉ & Rayaz A. Malik<sup>5,6</sup>

Parkinson's disease (PD) is characterized by progressive degeneration of dopaminergic neurons in the substantia nigra, while secondary parkinsonism (SP) may be due to drugs, vascular, infectious, inflammatory, or even paraneoplastic etiologies. There is currently no biomarker that accurately distinguishes SP from PD. Corneal confocal microscopy (CCM) identifies corneal nerve loss which is associated with motor, cognitive and autonomic dysfunction in PD patients. This study enrolled participants with PD ( $n = 45$ ) and SP ( $n = 25$ ). A subset of patients underwent L-6-<sup>18</sup>F-fluoro-3,4-dihydroxyphenylalanine (<sup>18</sup>F-DOPA) positron emission tomography (PET) scan which showed bilateral decreased dopamine uptake in the putamen and caudate of patients with PD, but not in those with SP. Corneal nerve fiber density (CNFD) ( $P < 0.001$ ) was lower and corneal nerve branch density (CNBD) ( $P = 0.007$ ) was higher in the PD group compared to the SP group. The receiver operating characteristic (ROC) analysis revealed that combined CNFD and CNBD showed excellent discrimination between SP and PD, with an area under the curve (AUC) of 0.924. CCM may have clinical utility in differentiating patients with SP from PD.

Parkinson's disease (PD) is characterized by progressive neurodegeneration of dopaminergic neurons in the substantia nigra and altered dopaminergic transmission leading to tremor, rigidity, bradykinesia and non-motor symptoms and signs<sup>1</sup>. Molecular imaging techniques, such as L-6-<sup>18</sup>F-fluoro-3,4-dihydroxyphenylalanine (<sup>18</sup>F-DOPA) positron emission tomography (PET), which target dopamine synthesis capacity in substantia nigra neurons have been instrumental in visualizing deficits in dopaminergic transmission to aid in the diagnosis of PD<sup>2</sup>. Patients with secondary parkinsonism (SP) have similar neurological manifestations to PD, due to cerebrovascular disease, certain drugs, infection, inflammation, and autoimmune abnormalities, without primary impairment of the nigrostriatal pathway<sup>3–5</sup>. Distinguishing PD from SP is crucial to determine appropriate management and prognostication. Apart from <sup>18</sup>F-DOPA PET, which is not widely available, there is currently no validated biomarker that accurately distinguishes SP from PD.

PD is a multisystem disease and studies have found peripheral nerve abnormalities<sup>6</sup> in large-medium (A $\alpha$ / $\beta$ ) and small (A $\delta$  and C) nerve fibers in PD<sup>7,8</sup>. Large fiber dysfunction has been attributed to levodopa therapy, while small fiber damage is thought to be intrinsic to the neurodegenerative process in PD<sup>8,9</sup>. Using corneal confocal microscopy (CCM), an in vivo ophthalmic imaging technique, we and others have demonstrated corneal nerve loss which was associated with the severity of motor<sup>10</sup>, cognitive and autonomic<sup>11,12</sup> dysfunction. Moreover, CCM has also been shown to differentiate different motor subtypes of PD<sup>13</sup>. In the present study, we utilized CCM to evaluate corneal nerve fiber damage in participants with SP and PD.

## Results

### Clinical and demographic profiles

A total of 53 PD patients were evaluated of whom 45 were included in this study. Among the 8 patients excluded, five had impaired glucose tolerance,

<sup>1</sup>Department of Neurology, People's Hospital of Zhengzhou University, School of Clinical Medicine, Zhengzhou University, Zhengzhou, China. <sup>2</sup>Department of Neurology, Henan Provincial People's Hospital, School of Clinical Medicine, Henan University, Zhengzhou, China. <sup>3</sup>School of Nursing, China Medical University, Shenyang, China. <sup>4</sup>Department of Neurology, the First Affiliated Hospital of Zhengzhou University, Zhengzhou, China. <sup>5</sup>Department of Medicine, Weill Cornell Medicine-Qatar, Doha, Qatar. <sup>6</sup>Division of Cardiovascular Sciences, School of Medical Sciences, University of Manchester, Manchester, UK. <sup>7</sup>These authors contributed equally: Hong-Qi Yang, Ran Xin, Ning-Ning Che. ✉e-mail: [ericnyng@163.com](mailto:ericnyng@163.com); [zhangjw9900@126.com](mailto:zhangjw9900@126.com)



two were multiple system atrophy (MSA) and one with corneal disease. The age of the PD group (62% male) was  $62.58 \pm 7.75$  years with a disease duration of 4 (2.5, 6.5) years. The average Hoehn and Yahr (H-Y) stage was 3 (2.0, 3.5).

For 32 patients with SP enrolled, 25 (11 drug-induced parkinsonism and 14 vascular parkinsonism) were finally included. Two post-encephalitic parkinsonism, 2 anti-NMDA-receptor encephalitis, 2 patients with normal pressure hydrocephalus, and 1 neurosyphilis were excluded. The age of the SP group (56% male) was  $64.00 \pm 7.23$  years with a disease duration of 3 (2, 5.5) years. The average H-Y stage was 3 (1, 3).

In the healthy control group ( $n = 30$ ), 53% were male, with an age of  $62.43 \pm 6.16$  years.

For the 11 drug-induced parkinsonism, the most common offending drugs were reserpine ( $n = 4$ , mean 18 (6 ~ 52) months), followed by haloperidol ( $n = 2$ , 10 and 36 months), flunarizine ( $n = 2$ , 24 and 46 months) and one each of risperidone (34 months), olanzapine (36 months) and citalopram (62 months). After discontinuation of the offending drugs, the majority of patients exhibited improvement in symptoms within 6 months. However, one patient's clinical profile remained unchanged following drug discontinuation, and she responded moderately to levodopa administration.

The 14 patients with vascular parkinsonism had an insidious onset of symptoms with a heterogenous presentation, including lower body parkinsonism ( $n = 9$ ), shuffling gait ( $n = 5$ ), asymmetric parkinsonism ( $n = 2$ ), and freezing of gait ( $n = 2$ ). Approximately half of the patients also showed wide-based gait, stooped posture, urinary incontinence, bulbar paralysis, pyramidal sign, and cognitive impairment. Tremor was relatively uncommon ( $n = 4$ ). The responses to levodopa were poor ( $n = 3$ ), moderate ( $n = 4$ ), or transient ( $n = 3$ ) with 4 showing a satisfactory response.

Brain magnetic resonance imaging (MRI) showed bilateral deep white matter lesions and periventricular white matter lesions in all patients. There was an enlargement of ventricles in two patients but the clinical profiles were not consistent with normal pressure hydrocephalus.

The part one of the Movement Disorders Society Unified Parkinson's Disease Rating Scale (MDS-UPDRS-I) ( $t = 2.475$ ,  $P = 0.013$ ) and the scale for outcomes in Parkinson's disease for autonomic symptoms (SCOPA-AUT) ( $t = 3.320$ ,  $P = 0.001$ ) were lower, while the olfactory test score was higher ( $t = 6.542$ ,  $P < 0.001$ ) in the SP group compared to the PD group (Table 1). There were no significant differences in age, sex, disease duration,

H-Y scores, MDS UPDRS-II scores, MDS UPDRS-III scores, and Montreal cognitive assessment (MoCA) between the two groups (Table 1).

### Presynaptic dopaminergic dysfunction

$^{18}\text{F}$ -fluorodeoxyglucose ( $^{18}\text{F}$ -FDG) and  $^{18}\text{F}$ -DOPA PET was performed in 10/30 controls, 25/45 participants with PD and 15/25 participants with SP (6 drug-induced parkinsonism and 9 vascular parkinsonism). In PD patients, visual assessment of the  $^{18}\text{F}$ -DOPA PET scan showed bilateral decreased dopamine uptake in the putamen and caudate which was more severe on the side contralateral to the clinically more affected side, in the posterior rather than anterior putamen, and was more severe in the putamen than the caudate. There was no evidence of decreased dopamine uptake in the putamen and caudate in participants with SP and controls. The representative brain MRI,  $^{18}\text{F}$ -FDG and corresponding  $^{18}\text{F}$ -DOPA PET image in each group are illustrated in Fig. 1.

Quantitative analysis of the  $^{18}\text{F}$ -DOPA PET signal was performed. Decreased striatal  $^{18}\text{F}$ -FDOPA uptake observed in patients with PD has been found to be most pronounced in the putamen compared to other striatal subregions like the caudate nucleus and ventral striatum<sup>14</sup>, thus the putamen was used as the ROI for the analysis. The putamen striatum to occipital lobe uptake ratio (SOR) was significantly lower in patients with PD compared to controls ( $2.22 \pm 0.55$  vs  $4.28 \pm 0.26$ ,  $P < 0.001$ ) and patients with SP ( $2.22 \pm 0.55$  vs  $3.97 \pm 0.44$ ,  $P < 0.001$ ), with no difference between the SP and control group.

### CCM between PD and SP

Corneal nerve fiber density (CNFD) ( $\text{no./mm}^2$ ) was significantly lower in the PD group compared to controls ( $24.88 \pm 4.77$  vs  $34.33 \pm 3.78$ ;  $P < 0.001$ ), did not differ between the SP group and controls ( $31.39 \pm 5.46$  vs  $34.33 \pm 3.78$ ;  $P = 0.069$ ) and was significantly lower in the PD group compared to SP group ( $24.88 \pm 4.77$  vs  $31.39 \pm 5.46$ ;  $P < 0.001$ ). Corneal nerve branch density (CNBD) ( $\text{no./mm}^2$ ) was higher in the PD group compared to controls ( $33.27 \pm 14.52$  vs  $24.58 \pm 8.23$ ;  $P = 0.004$ ), did not differ between the SP group and control group ( $24.59 \pm 5.89$  vs  $24.58 \pm 8.23$ ;  $P = 1.00$ ) and was significantly lower in the SP group compared to the PD group ( $24.59 \pm 5.89$  vs  $33.27 \pm 14.52$ ;  $P = 0.007$ ). Corneal nerve fiber length (CNFL) ( $\text{mm/mm}^2$ ) was significantly lower in the PD group compared to controls ( $14.23 \pm 3.39$  vs  $15.86 \pm 2.27$ ;  $P = 0.04$ ), with no difference between the SP and control group, nor between the SP and PD groups. Representative morphology of

**Table 1 | Demographic characteristics of participants**

	HC ( $n = 30$ )	PD ( $n = 45$ )	SP ( $n = 25$ )	P
Age, years	$62.43 \pm 6.16$	$62.58 \pm 7.75$	$64.00 \pm 7.23$	0.705
Sex M/F	16/14	28/17	14/11	0.743
Disease duration, years	NA	4 (2.5, 6.5)	3 (2, 5.5)	0.226
H-Y Stage	NA	3 (2.0, 3.5)	3 (1, 3.0)	0.751
LEDD (mg)	NA	475 (387.50, 643.75)	$465.00 \pm 156.62$	0.177
MDS UPDRS-I (score)	NA	$11.00$ (8.5, 17.5)	$9.12 \pm 4.01$	0.013
MDS UPDRS-II (score)	NA	$16.39 \pm 7.88$	$13.25 \pm 7.13$	0.108
MDS UPDRS-III (score)	NA	$35.91 \pm 18.58$	$30.92 \pm 15.51$	0.792
SCOPA-AUT (score)	NA	$16.07 \pm 7.42$	$10.48 \pm 5.30$ b**	0.001
MoCA (score)	NA	$20.56 \pm 6.07$	$23.00$ (16, 27.5)	0.397
Olfactory testing (score)	NA	$4.60 \pm 2.22$	$8.28 \pm 2.32$ b***	<0.001
CNFD $\text{no./mm}^2$	$34.33 \pm 3.78$	$24.88 \pm 4.77$ a***	$31.39 \pm 5.46$ b***	<0.001
CNBD $\text{no./mm}^2$	$24.58 \pm 8.23$	$33.27 \pm 14.52$ a**	$24.59 \pm 5.89$ b*	0.004
CNFL $\text{mm/mm}^2$	$15.86 \pm 2.27$	$14.23 \pm 3.39$ a*	$14.23 \pm 1.79$	0.192

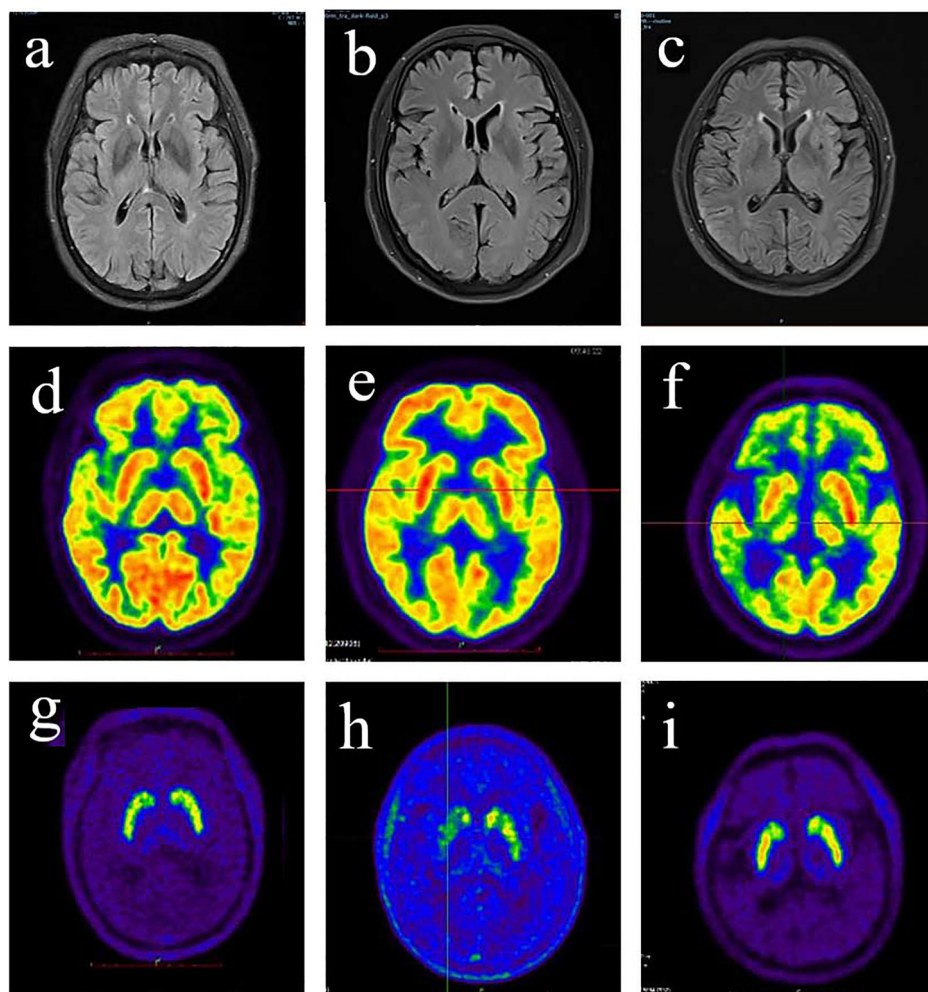
NA not available, PD Parkinson's disease, SP secondary parkinsonism, LEDD levodopa equivalent daily dose, MDS UPDRS Movement Disorders Society unified Parkinson's disease rating scale, SCOPA-AUT the scale for outcomes in PD for autonomic symptoms, MoCA Montreal cognitive assessment, CNFD corneal nerve fiber density, CNBD corneal nerve branch density, CNFL corneal nerve fiber length. (\* $P < 0.05$ , \*\* $P < 0.01$ , \*\*\* $P < 0.001$ ).

a: Controls vs PD.

b: PD vs SP.

**Fig. 1 | Representative images in each group.**

Images of MRI (a–c),  $^{18}\text{F}$ -FDG (d–f) and  $^{18}\text{F}$ -DOPA PET scans (g–i) in a healthy control (a, d, g), PD (b, e, h) and SP (c, f, i) patient. In a 65-year-old female PD patient who presented with 6 months of resting tremor, bradykinesia, muscle stiffness in the left side of the body, the cerebral MRI is basically normal (b), striatum glucose metabolism is increased bilaterally (e) and nigrostriatal degeneration is more affected in the right side than the left, and more impaired in the putamen than the caudate (h). In a SP participant with vascular parkinsonism who presented with shuffling gait, bradykinesia, bulbar paralysis and left pyramidal signs, axial cerebral MRI showed paraventricular high signal intensity predominantly in the right side consistent with a cerebral infarct 4 years ago. Cerebral  $^{18}\text{F}$ -FDG PET shows reduced metabolism in the right temporal lobe, parietal lobe, occipital lobe, thalamus and basal ganglia (f), which is in accordance with the cerebral infarction. In contrast to PD,  $^{18}\text{F}$ -DOPA PET uptake is relatively normal (i) indicating an intact nigrostriatal pathway.  $^{18}\text{F}$ -FDG:  $^{18}\text{F}$ -fluorodeoxyglucose,  $^{18}\text{F}$ -DOPA L-6- $^{18}\text{F}$ -fluoro-3,4-dihydroxyphenylalanine, PD Parkinson's disease, SP secondary parkinsonism.



the corneal nerve fibers and scatterplots of the individual CCM parameters in each group are shown in Figs. 2 and 3, respectively.

**Diagnostic utility of CCM**

ROC analysis showed that the area under the curve (AUC) distinguishing SP from PD for UPDRS-I, SCOPA-AUT and olfactory test was 0.679 (95% CI, 0.553–0.805), 0.728 (95% CI, 0.608–0.847) and 0.866 (95% CI, 0.777–0.955) respectively. Combining all three parameters resulted in an increased AUC of 0.907 (95% CI, 0.834–0.980) with a sensitivity and specificity of 72% and 97.8% respectively. The AUC distinguishing SP from PD for CNFD and CNBD was 0.817 (95% CI, 0.718–0.917) and 0.698 (95% CI, 0.576–0.821) respectively. Combining both CNFD and CNBD increased the AUC to 0.924 (95% CI, 0.860–0.988) with a sensitivity and specificity of 80% and 93.3%, respectively. Combining the clinical measures with CCM parameters further increased the AUC to 0.965 (95% CI, 0.909–1.000), with a sensitivity of 92% and specificity of 97.8% (Fig. 4).

**Correlation analysis between CCM and clinical measures**

Correlation analysis showed that CNFD and CNBD correlated positively with the olfactory test and negatively with SCOPA-AUT in PD patients (Fig. 5). CNFD ( $r = -0.277$ ,  $P = 0.065$ ) and CNBD ( $r = -0.291$ ,  $P = 0.051$ ) showed a trend towards a negative correlation with MDS UPDRS-I scores. There was no significant correlation between CNFD, CNBD, and clinical characteristics in patients with SP (Supplementary Fig. 1).

In PD, the SORs of the putamen correlated positively with CNFD ( $r = 0.668$ ,  $P = 0.003$ ) and CNBD ( $r = 0.768$ ,  $P < 0.001$ ). There was no significant correlation between SORs of the putamen and CCM parameters in the SP group (Supplementary Fig. 2).

**Discussion**

This study demonstrates a distinct pattern of corneal nerve fiber and  $^{18}\text{F}$ -DOPA PET alterations which differentiate patients with SP compared to PD. Furthermore, the ROC analysis reveals an excellent AUC for combined corneal nerve and clinical measures differentiating patients with SP from PD.

We have previously shown a lower CNFD and higher CNBD in patients with PD compared to controls<sup>10,11</sup>, indicating concomitant neuronal degeneration and regeneration<sup>7</sup>. We and others have also demonstrated corneal nerve loss in PD, especially in those with greater motor progression<sup>10</sup> and cognitive<sup>11</sup>, and autonomic dysfunction<sup>12</sup>. Additionally, corneal nerve morphology differed between motor subtypes of PD<sup>13</sup>, although it did not differ between PD patients with and without restless leg syndrome<sup>15</sup>. Our recent study also showed a lower CNFD, CNBD and CNFL in MSA patients with only a lower CNFD in patients with progressive supranuclear palsy (PSP)<sup>16</sup> and Niu et al. also showed lower CNFD and CNFL but comparable CNBD in patients with MSA compared to PD<sup>17</sup>.

In this study, despite similar clinical symptoms and signs, we show relative preservation of corneal nerve parameters and no evidence of pre-synaptic dopaminergic dysfunction on  $^{18}\text{F}$ -DOPA PET in patients with SP compared to PD<sup>2,18</sup>. Corneal nerve loss could serve as a surrogate marker for nigrostriatal dopaminergic dysfunction, though the precise basis for this requires further study.

Currently, there are no biomarkers to differentiate SP from PD. Our findings suggest that CCM has clinical utility in diagnosing and differentiating patients with SP from PD, with important consequences for management and predicting outcomes. The signs and symptoms of SP and PD are often very similar, neither motor nor non-motor symptoms effectively distinguish patients with SP from PD. Some studies have shown that



**Fig. 2 | Representative CCM images in each group.** CCM images in healthy controls (a, d, g), PD (b, e, h) and SP (c, f, i). The corneal nerve plexus is beaded, linear homogeneous and highly reflective (a–c). Nerve fiber trunks are highlighted in red; branch origins are represented by the green dots (d–f) and corneal nerve fiber length is shown in green line (g–i). Images (d–f) were analyzed with the manual software (CCMetrics) and images g–i were marked with the automated version (ACCMetrics). Scale bar=100  $\mu$ m. CCM corneal confocal microscopy, PD Parkinson's disease, SP secondary parkinsonism.

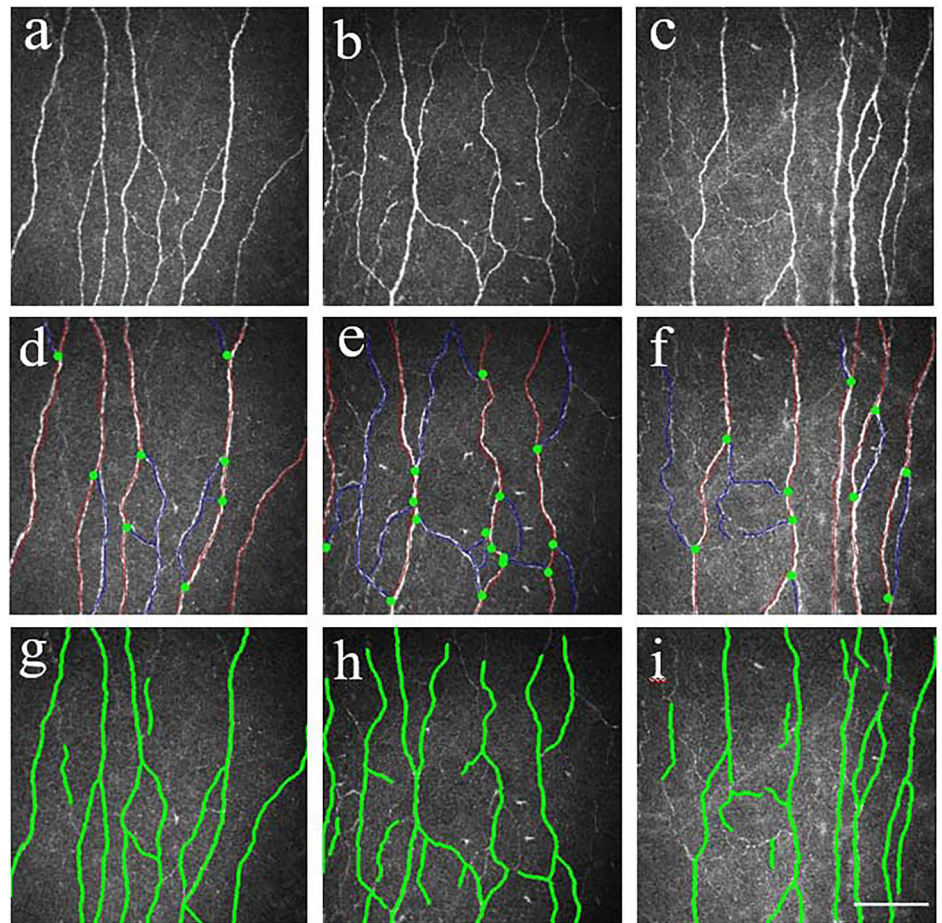
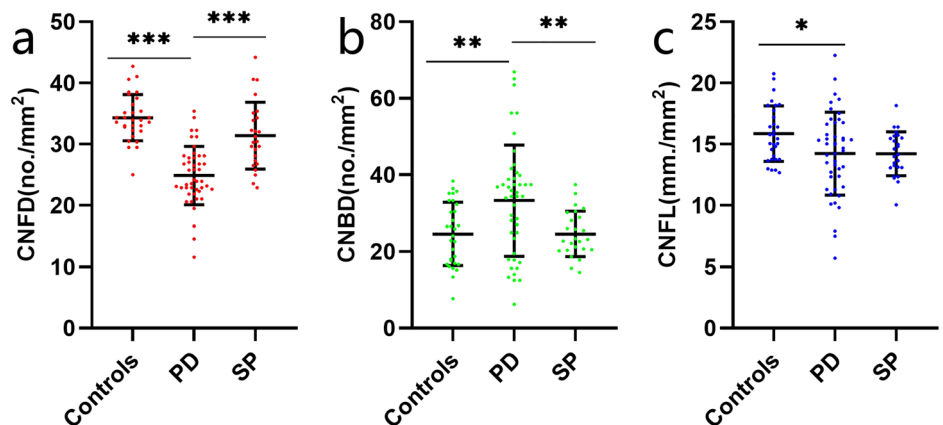


**Fig. 3 | CCM parameters in controls, PD patients and SP group.** CNFD (a), CNBD (b) and CNFL (c) in each group were compared with controls and dot plots were generated. CCM parameters in controls, PD patients and SP group (a–c). Errors bars represent mean  $\pm$  standard deviation (\* $P < 0.05$ , \*\* $P < 0.01$ , \*\*\* $P < 0.001$ ). PD Parkinson's disease, SP secondary parkinsonism, CCM corneal confocal microscopy, CNFD corneal nerve fiber density, CNBD corneal nerve branch density, CNFL corneal nerve fiber length.



the olfactory test may differentiate drug-induced parkinsonism from idiopathic PD<sup>19,20</sup>, and indeed we show a good correlation between abnormal corneal nerve parameters and the severity of olfactory dysfunction. Molecular imaging investigations like the DAT scan and/or cardiac <sup>123</sup>I-MIBG scintigraphy may also differentiate SP from PD<sup>21,22</sup>, but are costly and not readily available. We now show high sensitivity and specificity for corneal nerve parameters, especially when combined with clinical measures in differentiating patients with SP from PD.

The limitations of this study include the small sample size, especially as only a small portion of SP patients underwent the <sup>18</sup>F-DOPA PET scan. SP also has various etiologies, and our study only included patients with vascular and drug-induced parkinsonism. Given the relatively short follow-up

period of 12 months, a longer follow-up and repeated <sup>18</sup>F-DOPA PET scans may be necessary to exclude preclinical PD in the SP group<sup>23</sup>. Corneal nerve loss also occurs in a range of other neurodegenerative diseases including Alzheimer's disease<sup>24</sup>, Wilson disease<sup>25</sup>, Friedreich's ataxia<sup>26</sup>, multiple sclerosis<sup>27</sup> and amyotrophic lateral sclerosis<sup>28</sup>, impacting on its specificity. Thus, CCM alone is not sufficient for diagnosing and differentiating patients with SP, but requires consideration of clinical characteristics, imaging, treatment response to dopaminergic drugs, and exclusion of other causes.

In conclusion, patients with SP show preserved corneal nerve fibers and nigrostriatal function as compared to PD. CCM may have clinical utility as a rapid ophthalmic neuroimaging method for distinguishing patients with SP from PD.

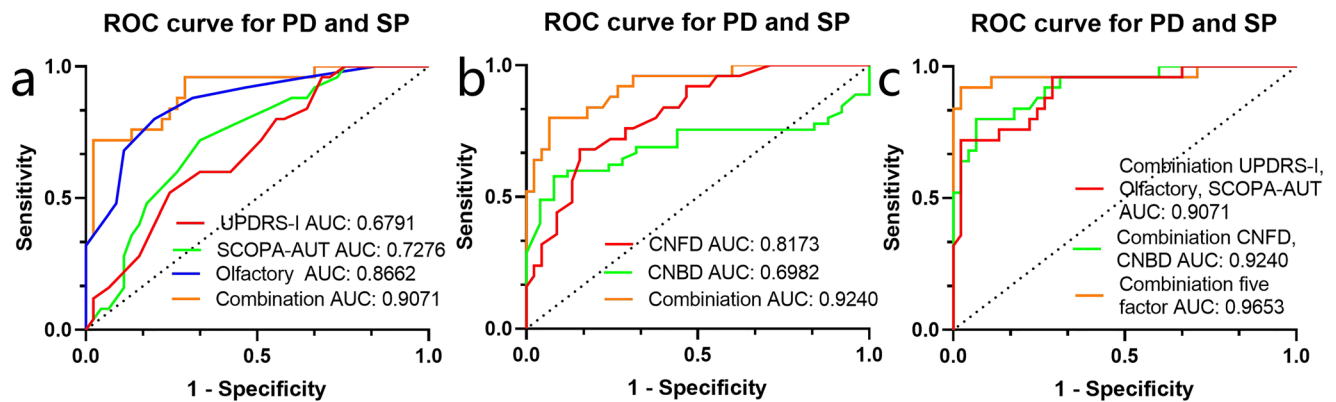


**Fig. 4 | The ROC for neurological measures and CCM in distinguishing SP from PD.** Clinical profile (a), CCM (b) and their combination (c) in distinguishing SP from PD. PD Parkinson's disease, SP secondary parkinsonism, CCM

corneal confocal microscopy, CNFD corneal nerve fiber density, CNBD corneal nerve branch density, ROC receiver operating characteristic, AUC under the curve.

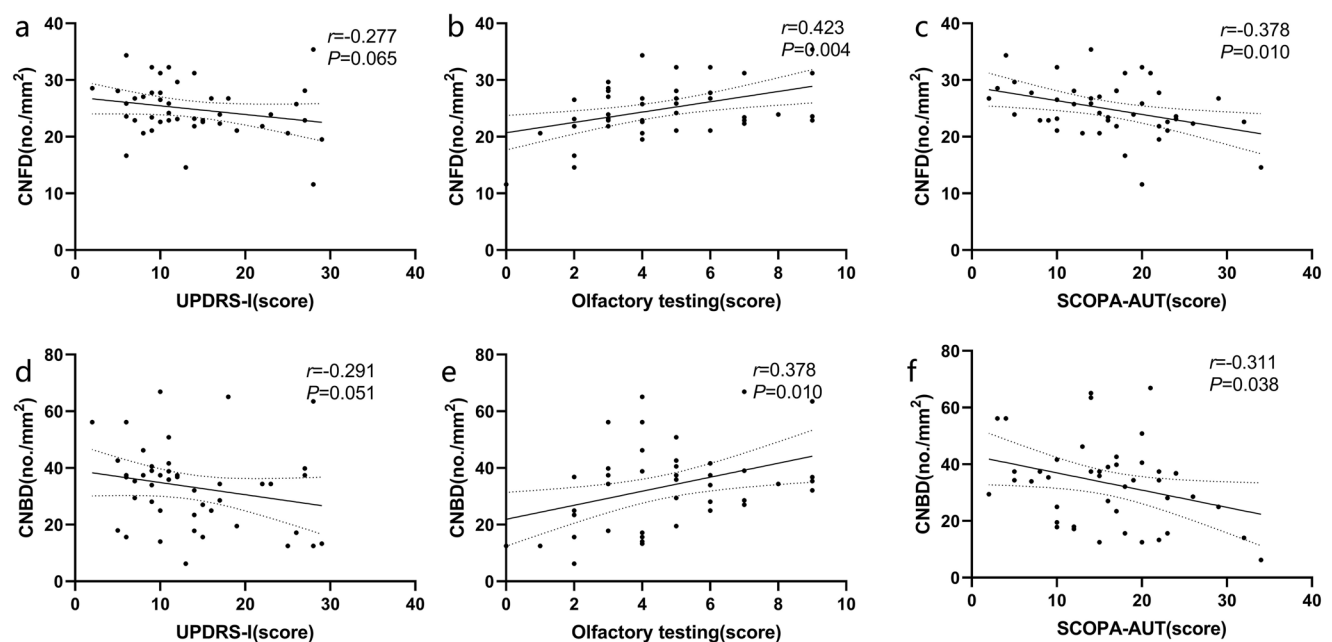


**Fig. 5 | Correlation between CCM and clinical profiles in PD patients.** Correlation plots and standardized correlation coefficient between clinical characteristics and CNFD (a–c) and CNBD (d–f). CCM corneal confocal microscopy, CNFD corneal nerve fiber density, CNBD corneal nerve branch density.

## Materials and Methods

### Participants

Participants were recruited from the Department of Neurology, Henan Provincial People's Hospital between March 2018 and December 2023. PD was diagnosed according to the 2015 Movement Disorder Society clinical diagnostic criteria for Parkinson's disease<sup>29</sup> and participants with clinically diagnosed and clinically probable PD were recruited. Parkinson-plus syndromes such as MSA, PSP, cortical basal ganglia degeneration (CBD), dementia with Lewy bodies (DLB) and those with a family history of a movement disorder were excluded from the study.

Drug-induced parkinsonism was diagnosed<sup>30</sup> by the presence of parkinsonism (at least two symptoms of either bradykinesia, tremor, or rigidity) after commencing the drug and after excluding other neurodegenerative etiologies. Participants were followed-up for at least 12 months to rule out a neurodegenerative etiology.

Vascular parkinsonism was diagnosed according to the following criteria<sup>33</sup>: presence of parkinsonism; evidence of cerebrovascular disease indicated by clinical symptoms/signs, MRI lesions, or both; parkinsonism

could be acute or insidious onset, within one year of cerebrovascular disease manifestations.

Other causes of SP such as infectious, immune-mediated, normal pressure hydrocephalus, or traumatic were excluded from the study.

Healthy controls were recruited from volunteers or spouses of PD patients with no history of neurodegenerative disease. Subjects younger than 40 or older than 85 years of age were excluded from the study. Subjects with a history of corneal disease, eye surgery, glaucoma, eye inflammation, or thyroid eye disease were excluded. Other causes of peripheral neuropathy were excluded based on a history of excess alcohol use (>150 mL/d) and an assessment of vitamin B<sub>12</sub> and folate, serum electrophoresis to exclude multiple myeloma, cryoglobulinemia and macroglobulinemia and an oral glucose tolerance test to exclude impaired glucose tolerance and diabetes. All subjects agreed to participate in the study and written informed consent was obtained. The clinical features of each participant were carefully evaluated by an experienced neurologist (H.-Q. Yang) who was specialized in PD and related movement disorders. The study was approved by the ethics committee of Henan Provincial People's Hospital (No. 202148).

## Clinical evaluation

The assessment of motor and non-motor symptoms was performed in the “ON” state in PD patients. PD symptoms were assessed with part I, II, III and IV sub-scales of the MDS-UPDRS and H-Y staging was undertaken for all PD patients<sup>31</sup>. Age at onset was defined as the time of the first cardinal motor sign(s), noted by either the patient or family members. Disease duration was defined as the time interval between presentation with first motor symptoms and enrollment into the present study. The SCOPA-AUT, a reliable and validated questionnaire that evaluates autonomic dysfunction was undertaken in patients with PD to detect autonomic dysfunction. MoCA was used to assess the cognitive status. Olfactory function was assessed with an olfactory kit for Parkinson’s disease (Jiangsu Parkinsense Biotech Co., Ltd, Nanjing, China). The olfactory kit consists of twelve smell cards, with four olfactory options each and the subject is required to choose the correct one. All subjects are required to complete all odor tests, and the result is represented by the overall score. Olfactory dysfunction was identified by a score <8<sup>10</sup>. Levodopa equivalent daily dose (LEDD) was assessed according to the levodopa conversion formula<sup>32</sup>. Briefly, 100 mg levodopa = 133 mg entacapone = 1 mg pramipexole = 5 mg ropinirole = 10 mg selegiline = 1 mg rasagiline = 100 mg amantadine.

## Neuroimaging investigations

All neuroimaging investigations were performed in the ON state. Participants underwent cerebral MRI with a Discovery MR750 scanner (GE Healthcare Bio-Sciences). T1-weighted, T2-weighted, fluid attenuated inversion recovery (FLAIR), and susceptibility-weighted imaging (SWI) sequences were included to rule out other diagnoses. <sup>18</sup>F-FDG and <sup>18</sup>F-DOPA PET were performed to assess cerebral metabolic activity and evaluate the functional integrity of the presynaptic dopaminergic pathway to assist in the diagnosis of PD and to differentiate it from atypical parkinsonism, as these disorders exhibit distinct patterns of dopaminergic and fluorodeoxyglucose metabolism<sup>33,34</sup>.

Prior to <sup>18</sup>F-FDG PET examination, patients were required to fast for ≥6 h with a fasting blood glucose level of <6.1 mmol/l. Fifty minutes after intravenous injection of <sup>18</sup>F-FDG at a dose of 5.55 MBq/kg, <sup>18</sup>F-FDG PET images were obtained using a Discovery VCT PET-CT set (GE Healthcare Bio-Sciences). An acquisition counter using an iterative method was used to reconstruct transverse, sagittal and coronal images.

For <sup>18</sup>F-DOPA PET scanning, the drugs for PD were administrated as usual. <sup>18</sup>F-DOPA PET was performed 90 min after intravenous injection of <sup>18</sup>F-DOPA (370 MBq) and the PET acquisition time was 30 min. All PET scans were performed in the PET center of Henan Provincial People’s Hospital.

Quantitative analysis of <sup>18</sup>F-DOPA uptake was conducted by an experienced neurologist (S. Chen) who was blinded to the study design. The areas of interest (ROI) were drawn on the MR images and copied to the PET images to calculate the average radioactivity in 3 planes. The ROIs were located bilaterally at the striatum and the occipital cortex with the occipital cortex acting as a reference. The SOR was used as a quantitative measure of presynaptic dopaminergic function. SORs were generated for the striatum on each side and then averaged from occipital ROI data.

## Corneal confocal microscopy

A Heidelberg Retina Tomograph III with a Rostock Cornea Module (HRT III RCM; Heidelberg Engineering GmbH, Heidelberg, Germany) was used to acquire images of the central corneal sub-basal nerve plexus. To minimize the influence of motor symptoms, especially tremor, CCM was conducted in PD patients when they were in the “ON” state. Topical lidocaine was used to anesthetize the eye of each subject, who was then seated and instructed to focus on an outer fixation light. The TomoCap was correctly positioned on the cornea by visualizing with the CCD camera. An experienced examiner took images of the sub-basal nerve plexus in the central cornea using the “section” mode according to an established protocol<sup>35</sup>. 4–6 optimal quality CCM images from the central cornea of each eye were selected and analyzed using validated, manual (CCMetrics) and automated (ACCMetrics,

Imaging Science and Biomedical Engineering, Manchester, UK) purpose-written software<sup>36</sup>. Three parameters were analyzed in this study: (a) CNFD: the number of main nerve fibers per square millimeter; (b) CNBD: the number of primary branches originating from the main nerve; (c) CNFL: the sum of length of all nerve fibers per square millimeter.

## Statistical analysis

The Shapiro-Wilk test was used to assess the normality of data. Normally distributed variables are expressed as mean ± standard deviation (SD). Analysis of variance with Bonferroni as post hoc test and t-tests were used for group comparison. Non-normal or non-homoscedasticity variables are expressed as median (interquartile range). Multiple comparisons were performed with the non-parametric Kruskal-Wallis test. Chi-square tests and Fisher’s exact tests were used to compare categorical variables. Spearman or Pearson correlation analysis was performed to assess the association between corneal nerve fiber and clinical characteristics in the PD group. The receiver operating characteristic (ROC) curve was applied to analyze the capability of corneal nerve fiber parameters for discriminating PD and SP participants. All analyses were carried out using SPSS version 22.0 (IBM Corporation, Armonk, NY, USA). Scatter plots and ROC curves were generated using GraphPad Prism version 8.0 (GraphPad Software, Inc, San Diego, CA, USA). *P* < 0.05 was considered statistically significant.

## Data availability

The authors confirm that the data supporting the findings of this study are available within the article.

Received: 20 August 2024; Accepted: 14 April 2025;

Published online: 06 May 2025

## References

- Schapira, A. H. V., Chaudhuri, K. R. & Jenner, P. Non-motor features of Parkinson disease. *Nat. Rev. Neurosci.* **18**, 435–450 (2017).
- Eshuis, S. A. et al. Direct comparison of FP-CIT SPECT and F-DOPA PET in patients with Parkinson’s disease and healthy controls. *Eur. J. Nucl. Med Mol. Imaging* **36**, 454–462 (2009).
- Che, N. N., Chen, S. Y., Li, X., Ma, J. J. & Yang, H. Q. Autoimmune-mediated secondary-parkinsonism presented with micrographia and cognitive impairment. *J. Neuroimmunol.* **361**, 577738 (2021).
- Bondon-Guitton, E. et al. Drug-induced parkinsonism: a review of 17 years’ experience in a regional pharmacovigilance center in France. *Mov. Disord.* **26**, 2226–2231 (2011).
- Korczyn, A. D. Vascular parkinsonism-characteristics, pathogenesis and treatment. *Nat. Rev. Neurol.* **11**, 319–326 (2015).
- Ceravolo, R. et al. Neuropathy and levodopa in Parkinson’s disease: evidence from a multicenter study. *Mov. Disord.* **28**, 1391–1397 (2013).
- Che, N. N. & Yang, H. Q. Potential use of corneal confocal microscopy in the diagnosis of Parkinson’s disease associated neuropathy. *Transl. Neurodegener.* **9**, 28 (2020).
- Donadio, V. et al. Skin nerve α-synuclein deposits: a biomarker for idiopathic Parkinson disease. *Neurology* **82**, 1362–1369 (2014).
- Cossu, G. & Melis, M. The peripheral nerve involvement in Parkinson disease: a multifaceted phenomenon. *Parkinsonism Relat. Disord.* **25**, 17–20 (2016).
- Lim, S. H. et al. Corneal Confocal Microscopy Identifies Parkinson’s Disease with More Rapid Motor Progression. *Mov. Disord.* **36**, 1927–1934 (2021).
- Che, N. N. et al. Corneal nerve fiber loss relates to cognitive impairment in patients with Parkinson’s disease. *NPJ Parkinsons Dis.* **7**, 80 (2021).
- Che, N. N. et al. Corneal confocal microscopy differentiates patients with Parkinson’s disease with and without autonomic involvement. *NPJ Parkinsons Dis.* **8**, 114 (2022).
- Che, N. N. et al. The severity of corneal nerve loss differentiates motor subtypes in patients with Parkinson’s disease. *Ther. Adv. Neurol. Disord.* **16**, 17562864231165561 (2023).



14. Jokinen, P. et al. Simple ratio analysis of 18F-fluorodopa uptake in striatal subregions separates patients with early Parkinson disease from healthy controls. *J. Nucl. Med* **50**, 893–899 (2009).
15. Andréasson, M. et al. Parkinson's disease with restless legs syndrome—an in vivo corneal confocal microscopy study. *NPJ Parkinsons Dis.* **7**, 4 (2021).
16. Lim, S. H. et al. Corneal confocal microscopy demonstrates varying degrees of neurodegeneration in atypical parkinsonian disorders. *Parkinsonism Relat. Disord.* **117**, 105899 (2023).
17. Niu, X. et al. Corneal confocal microscopy may help to distinguish Multiple System Atrophy from Parkinson's disease. *NPJ Parkinsons Dis.* **10**, 63 (2024).
18. Thobois, S., Prange, S., Scheiber, C. & Broussolle, E. What a neurologist should know about PET and SPECT functional imaging for parkinsonism: A practical perspective. *Parkinsonism Relat. Disord.* **59**, 93–100 (2019).
19. Lee, P. H., Yeo, S. H., Yong, S. W. & Kim, Y. J. Odour identification test and its relation to cardiac 123I-metaiodobenzylguanidine in patients with drug induced parkinsonism. *J. Neurol. Neurosurg. Psychiatry* **78**, 1250–1252 (2007).
20. Katzenschlager, R., Zijlmans, J., Evans, A., Watt, H. & Lees, A. J. Olfactory function distinguishes vascular parkinsonism from Parkinson's disease. *J. Neurol. Neurosurg. Psychiatry* **75**, 1749–1752 (2004).
21. Brigo, F., Matinella, A., Erro, R. & Tinazzi, M. [<sup>123</sup>I]FP-CIT SPECT (DaTSCAN) may be a useful tool to differentiate between Parkinson's disease and vascular or drug-induced parkinsonisms: a meta-analysis. *Eur. J. Neurol.* **21**, 1369–e90 (2014).
22. Brigo, F., Erro, R., Marangi, A., Bhatia, K. & Tinazzi, M. Differentiating drug-induced parkinsonism from Parkinson's disease: an update on non-motor symptoms and investigations. *Parkinsonism Relat. Disord.* **20**, 808–814 (2014).
23. Rektor, I. et al. An updated diagnostic approach to subtype definition of vascular parkinsonism - Recommendations from an expert working group. *Parkinsonism Relat. Disord.* **49**, 9–16 (2018).
24. Ponirakis, G. et al. Loss of corneal nerves and brain volume in mild cognitive impairment and dementia. *Alzheimers Dement (N.Y.)*. **8**, e12269 (2022).
25. Sturniolo, G. C. et al. Small fiber peripheral neuropathy in Wilson disease: an in vivo documentation by corneal confocal microscopy. *Invest Ophthalmol. Vis. Sci.* **56**, 1390–1395 (2015).
26. Pagovich, O. E. et al. Corneal confocal microscopy: Neurologic disease biomarker in Friedreich ataxia. *Ann. Neurol.* **84**, 893–904 (2018).
27. Bitirgen, G., Akpinar, Z., Malik, R. A. & Ozkagnici, A. Use of Corneal Confocal Microscopy to Detect Corneal Nerve Loss and Increased Dendritic Cells in Patients With Multiple Sclerosis. *JAMA Ophthalmol.* **135**, 777–782 (2017).
28. Fu, J. et al. Small fiber neuropathy for assessment of disease severity in amyotrophic lateral sclerosis: corneal confocal microscopy findings. *Orphanet J. Rare Dis.* **17**, 7 (2022).
29. Postuma, R. B. et al. MDS clinical diagnostic criteria for Parkinson's disease. *Mov. Disord.* **30**, 1591–1601 (2015).
30. López-Sendón, J., Mena, M. A. & de Yébenes, J. G. Drug-induced parkinsonism. *Expert Opin. Drug Saf.* **12**, 487–496 (2013).
31. Goetz, C. G. et al. Movement Disorder Society-sponsored revision of the Unified Parkinson's Disease Rating Scale (MDS-UPDRS): scale presentation and clinimetric testing results. *Mov. Disord.* **23**, 2129–2170 (2008).
32. Tomlinson, C. L. et al. Systematic review of levodopa dose equivalency reporting in Parkinson's disease. *Mov. Disord.* **25**, 2649–2653 (2010).
33. Meyer, P. T., Frings, L., Rücker, G. & Hellwig, S. <sup>18</sup>F-FDG PET in Parkinsonism: Differential Diagnosis and Evaluation of Cognitive Impairment. *J. Nucl. Med* **58**, 1888–1898 (2017).
34. Broski, S. M. et al. Structural and functional imaging in parkinsonian syndromes. *Radiographics* **34**, 1273–1292 (2014).
35. Tavakoli M., Malik R. A. Corneal confocal microscopy: a novel non-invasive technique to quantify small fibre pathology in peripheral neuropathies. *J Vis Exp.* <https://doi.org/10.3791/2194> (2011)
36. Tavakoli, M. et al. Normative values for corneal nerve morphology assessed using corneal confocal microscopy: a multinational normative data set. *Diabetes Care* **38**, 838–843 (2015).

## Acknowledgements

We thank the patients and healthy individuals for their participation in this study. We also thank the Manchester Biomedical Research Centre for access to the CCMetrics and ACCMetrics software. The study was funded by Henan Provincial Natural Science Foundation (242300421289). The funding bodies did not participate in the study design, in data collection, analysis, and interpretation, and in writing the manuscript.

## Author contributions

H.-Q. Yang, R. Xin and N.-N. Che made equal contributions to conception and design, acquisition of data, and drafting the manuscript. H.-Q. Yang undertook supervision of the research group and was involved in critically revising the manuscript. Q.-H. Jiang, S. Chen, S.-Y. Chen, Z.-K. Sun, and W.-M. Yang participated in data collection. X. Li, J.-J. Ma, and J.-W. Zhang contributed to the interpretation of the data. RA Malik helped critically revise the manuscript. All authors read and approved the final manuscript.

## Competing interests

The authors declare no competing interests.

## Additional information

**Supplementary information** The online version contains supplementary material available at <https://doi.org/10.1038/s41531-025-00969-2>.

**Correspondence** and requests for materials should be addressed to Hong-Qi Yang or Jie-Wen Zhang.

**Reprints and permissions information** is available at <http://www.nature.com/reprints>

**Publisher's note** Springer Nature remains neutral with regard to jurisdictional claims in published maps and institutional affiliations.

**Open Access** This article is licensed under a Creative Commons Attribution-NonCommercial-NoDerivatives 4.0 International License, which permits any non-commercial use, sharing, distribution and reproduction in any medium or format, as long as you give appropriate credit to the original author(s) and the source, provide a link to the Creative Commons licence, and indicate if you modified the licensed material. You do not have permission under this licence to share adapted material derived from this article or parts of it. The images or other third party material in this article are included in the article's Creative Commons licence, unless indicated otherwise in a credit line to the material. If material is not included in the article's Creative Commons licence and your intended use is not permitted by statutory regulation or exceeds the permitted use, you will need to obtain permission directly from the copyright holder. To view a copy of this licence, visit <http://creativecommons.org/licenses/by-nc-nd/4.0/>.

© The Author(s) 2025